Journal of Catalysis **182,** 30–36 (1999)
Article ID jcat.1998.2313, available online at http://www.idealibrary.com on IDEAL®

Stability and Surface Catalytic Properties of Fluorite-Structured Yttria-Doped Bismuth Oxide under Reducing Environment

Y. Zeng[1] and Y. S. Lin[2]

Department of Chemical Engineering, University of Cincinnati, Cincinnati, Ohio 45221-0171

Received March 24, 1998; revised August 13, 1998; accepted August 17, 1998

High temperature stability and catalytic properties of fluorite-type 25 mol% Y_2O_3 doped Bi_2O_3 (BY25) pellets under methane atmosphere were studied by XRD, transient TGA and fixed-bed reactor measurements. In methane the fluorite-type BY25 exhibits good catalytic properties for oxidative coupling of methane (OCM) with C_2 selectivity higher than 90% and C_2 formation rate in the range of 1–3 μmol/g · s. BY25 maintains its fluorite-type phase structure and catalytic properties as long as only nonstoichiometric oxygen in BY25 is consumed (less than 20% of the total oxygen). Prolonged (>5–7 min) exposure of BY25 to methane results in consumption of stoichiometric oxygen, leading to reduction of metal ions and destruction of the fluorite structure of BY25. These results suggest that the stability and catalytic properties of the surface of the BY25 membrane exposed to methane stream in membrane reactor applications can be maintained if sufficient oxygen is provided from the other side of the membrane.

INTRODUCTION

Bi_2O_3 in the fluorite phase structure (δ-phase Bi_2O_3) exhibits considerable oxygen ionic conductivity at temperatures higher than 800°C, due to its defect structure with up to 25% oxygen sites vacant (1, 2). Because of its high ionic conductivity, δ-phase Bi_2O_3 has been considered as a potential electrolyte material for high temperature solid oxide fuel cells or oxygen sensors. δ-phase Bi_2O_3 doped with yttria also shows very attractive catalytic properties for oxidative coupling of methane (OCM) to ethane and ethylene (3, 4). Therefore, δ-phase Bi_2O_3 offers potential applications as a catalyst in a fixed-bed reactor (possibly operated in cyclic mode) or as a membrane in a membrane reactor for partial oxidative reaction of methane (3–6). Obviously, the phase and chemical stability of δ-phase Bi_2O_3 will be a critical issue in these applications.

Pure Bi_2O_3 can maintain its δ-phase between 810°C (melting point) and 730°C (transformation temperature to a monoclinic phase structure) (7). Earlier work showed that doping a certain amount of Y_2O_3 or some other oxides in Bi_2O_3 can stabilize the δ-phase to lower temperatures and raise the melting point of Bi_2O_3 to above 1000°C (7). However, Watanabe *et al.* (8) later pointed out that the stabilized δ-phases reported earlier were the quenched high-temperature stable phases which form a solid solution based on δ-Bi_2O_3. These quenched phases are meta-stable below a critical temperature (e.g., 700°C), which varies with composition and oxide additive. On annealing in 500–650°C for more than 100 h, doped Bi_2O_3 in the δ-phase transforms gradually to the low-temperature stable phases or decomposes into several other phases. These findings were later confirmed by Joshi *et al.* (9). The thermochemical stability of yttria-doped bismuth oxide was also investigated by Kruidhof *et al.* (10, 11). They found that the δ-phase can be stabilized to lower temperatures if more than 31.8 mol% yttria is doped in bismuth oxide.

The studies summarized above were focused on stability of the bismuth oxides with different dopants in oxygen atmosphere. Chemical and phase stability under reducing atmosphere and at temperatures higher than 800°C was not addressed in the previous studies. As part of our effort to identify suitable ceramic with desired catalytic and oxygen permeation properties for membrane reactor application, recently we found that BY ceramics in the fluorite structure (δ-Bi_2O_3 phase) is catalytic active and selective for OCM at 800°C (3, 4). In a cofeed fixed-bed reactor with a $CH_4 : O_2 : He$ ratio of 2.9 : 1 : 1.3, a C_2 yield of 18% and a C_2 selectivity of 60% were achieved on 25 mol% Y_2O_3-doped Bi_2O_3 (BY25) pellets. More importantly, BY25 offers the C_2 space-time yield for OCM about 15 times higher than one of the best catalysts for OCM (Li/MgO) (12). To further explore potential applications of the BY ceramics as catalyst or membrane in reactors for OCM, the stability of BY ceramics at temperature higher than 800°C and under reducing environment should be studied. The present paper reports results of the study.

[1] Current address: BOC Technical Center, 100 Mountain Ave., NJ 07974.

[2] To whom correspondence should be addressed.

0021-9517/99 $30.00

EXPERIMENTAL

25 mol% Y_2O_3-doped Bi_2O_3 (BY25) green powder was prepared by the oxalate (coprecipitation) method. In synthesis, corresponding metal nitrates, $Bi(NO_3)_3 \cdot 5H_2O$ (99.9%, Fisher) and $Y(NO_3)_3 \cdot 6H_2O$ (99.9%, Johnson Matthey), in desired proportion were dissolved into deionized water by adding 10 vol% concentrated nitric acid. This solution was then added dropwise into an oxalic acid solution while stirring. The above operations were conducted at room temperature. The corresponding oxalates were formed and precipitated as very fine particles from the solution. These white precipitates were collected (by filtration), dried at 120°C overnight and calcined subsequently at 600°C for 5–10 h. Thus prepared green powders were then packed in a stainless steel mold and hydraulically pressed into a disk which was sintered at a higher temperature (>800°C) for a period of time ranging from 5 to 20 h. BY25 pellets (1–3 mm in size) used in this work were prepared by crushing the BY25 disks. The phase structures of the catalysts were studied by X-ray diffraction (Siemens Kristalloflex D500 diffractometer, with Cu Kα radiation). The real and theoretical densities were measured by the Archimedes method and calculated from the lattice parameter (measured by XRD), respectively.

A packed-bed reactor was employed to study the OCM catalytic properties of BY25 pellets under methane atmosphere. The reactor was made of a dense alumina tube (0.63-cm ID, 56-cm long). The BY25 pellet sample in an amount of about 0.3 g was packed in the middle portion of the reactor tube and supported by quartz beads (0.5 mm in diameter) from both sides of the reactor tube. It was proved by blank experiments that both alumina tube and quartz particles were catalytically inert to the OCM reactions. In the fixed-bed experiments, the reactor tube was first heated up to 900°C in air flow. Before the methane run, pure oxygen was passed through the reactor for about 10 min to ensure that the BY sample was saturated with oxygen. Subsequently, pure helium was passed through the reactor for 30 s to purge out the gas phase oxygen before pure methane was introduced into reactor. The effluent from the reactor during methane run was intermittently sampled and analyzed by gas chromatography.

Instantaneous formation rates for product i at the time of sampling were calculated from the total effluent flow rate, M_{out}, and molar fraction, Y_j, as

$$R_j = M_{\text{out}} Y_j / m_{\text{cat}}, \qquad [1]$$

where m_{cat} is the amount of catalyst packed. The selectivity for carbon containing species was calculated from the effluent compositions by

$$S_j = n_j Y_j \big/ \left(\Sigma n_j Y_j - Y_{CH_4}\right), \qquad [2]$$

where n_j is number of carbon atom in molecule j.

Transient TGA experiments were carried out in a high temperature electronic recording microbalance system (Cahn 1000) (6). In experiments, about 0.8-g BY25 pellet sample was put in a quartz sample pan placed inside a vertical quartz reactor tube ($\phi = 5$ cm) of the balance. The sample was heated up from the room temperature to 900°C in pure oxygen. After the sample weight became constant at the desired temperature, the BY25 sample in the balance was subsequently exposed to the flows of helium, methane, and oxygen for given periods of time. The transient weight of the sample in different atmospheres was recorded by a PC data acquisition system. The flow rate of the stream fed to the balance reactor tube was 200 ml (STP)/min for O_2 and He and 50 ml (STP)/min for CH_4.

RESULTS AND DISCUSSION

The BY25 pellet samples prepared in this study were in the perfect fluorite-type face-centered cubic (fcc) phase structure as confirmed by XRD pattern shown in Fig. 1a. The average particle size of BY25 pellets used in this study was about 2 mm. The relative density, defined as the ratio of real density to the theoretical one, was 76%, indicating that the BY25 pellets were not completely dense. However, the density measured by Archimedes method using both mercury and water as the immersing liquid were identical, suggesting that the pores inside the BY25 bulk phase are close. The surface area of the samples is much

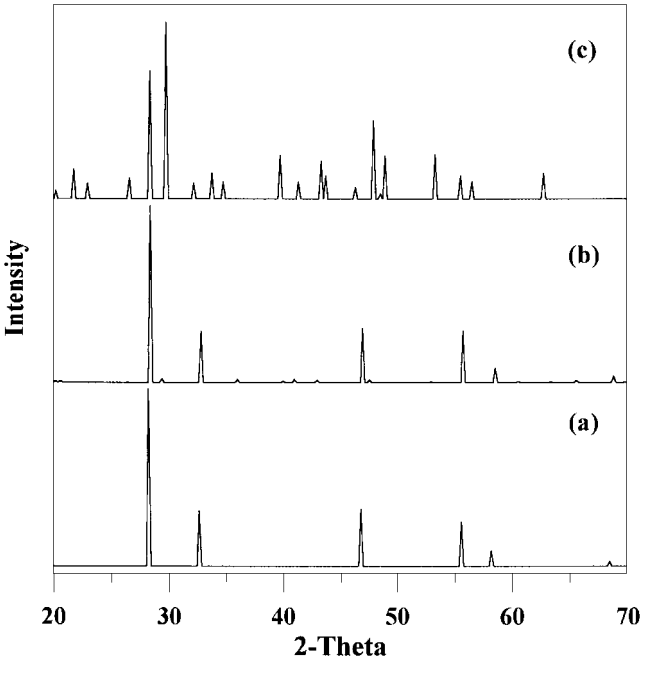

FIG. 1. XRD patterns of BY25 pellet used in fixed-bed reactor experiments: (a) fresh sample; (b) after 4 min methane run; and (c) after 28 min methane run.

smaller than 0.001 m^2/g. Experiments showed that the sample surface area and pore volume were too small to be measured by N_2 adsorption using a Micromeritics ASAP-2000 adsorption porosimeter. All experiment results reported next were measured at 900°C, with methane space time velocity of 3.5×10^{-3} g · min/ml for the fixed bed experiments. Since the catalytic properties of BY25 were sensitive to the particle size and surface area of the BY25 sample (3, 4), BY25 pellets from the same batch were used in the fixed bed and TGA experiments in this work.

In the fixed-bed experiments, the effluent from the reactor during methane contained primarily ethylene, ethane, methane, carbon dioxide, and water vapor. There was essentially no carbon monoxide found in the effluent. Figure 2 shows the C_2 selectivity, C_2 and CO_x formation rates and C_2H_4 to C_2 ratio for OCM on the BY25 pellets as a function of methane run time up to 28 min. At the given methane space velocity, the methane conversion was typically lower than 3%. As shown in Fig. 2, C_2 selectivity remained essentially unchanged at around 90%, indicating good intrinsic selectivity of the BY25 surface for C_2 formation reaction. The C_2 formation rate decreases rapidly in the first few minutes of the methane run. The C_2H_4 to C_2 ratio also decreases with methane run time.

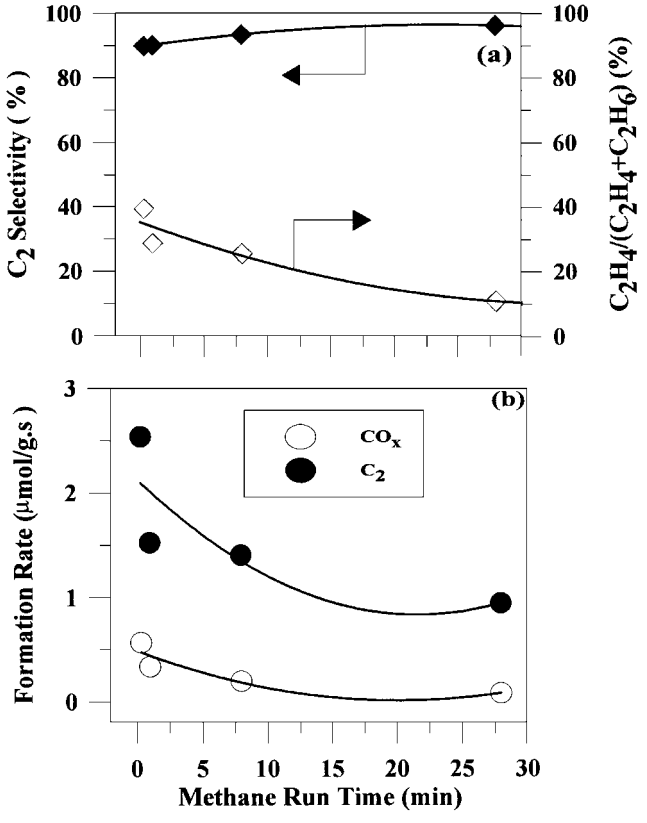

FIG. 2. C_2 selectivity, percentage of ethylene, and C_2 and CO_x formation rates as a function of methane run time over BY25 pellets under cyclic mode.

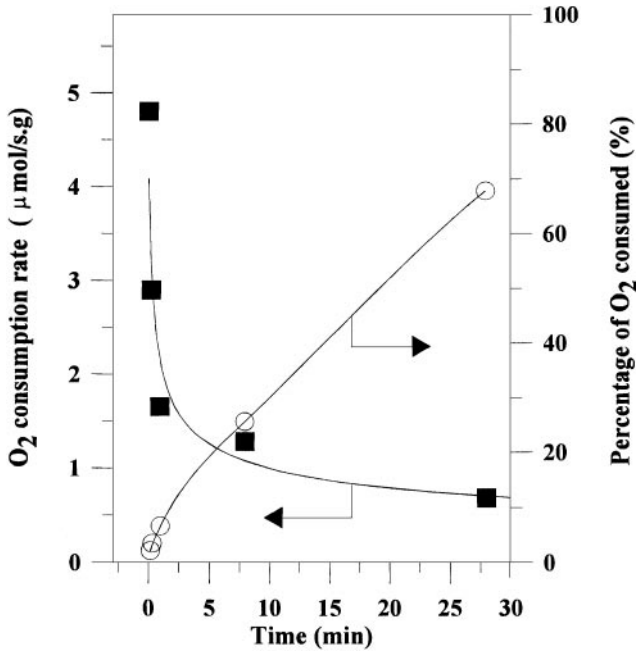

FIG. 3. Oxygen consumption rate and accumulated percentage of lattice oxygen consumed as a function of methane run time over BY25 pellet under cyclic mode.

The oxygen consumption rate of the BY25 pellets during the 28-min methane run was calculated from the formation rates of oxygen-containing species, i.e., CO_x and H_2O. The accumulated amount of oxygen consumed at a given methane run time, *t*, was then calculated by integrating the oxygen consumption rate from time zero to *t*. The initial amount of oxygen in the catalyst was estimated assuming that all oxygen sites of BY25 lattice were occupied by oxygen at 900°C and oxygen partial pressure of 1 atm. The results of the oxygen consumption rate and the percentage of oxygen consumed as a function of methane run time are given in Fig. 3.

As shown, the oxygen consumption rate exhibits an exponential decrease with methane run time, with a sharp change of about 3.5 μmol/s · g in the first 5 min. This time period corresponds to about 20% of oxygen in the BY25 pellets consumed, as shown in Fig. 3. XRD pattern of the BY25 pellets after 4 min methane run (measured at room temperature after the sample was quenched in air from the reactor) is shown in Fig. 1b. The sample remained essentially in the same fluorite phase structure as the fresh sample.

Continuous reaction over the BY pellets results in consumption of oxygen up to 63% of the total oxygen available in the BY sample at methane run time of 28 min. We observed a porous layer in light yellow color on the outer part of the BY25 pellet after the experiment. This layer could be easily peeled off. However, the center part of the pellets remained dense and in a color of dark yellow just like the fresh pellets. XRD pattern of the BY25 after the 28-min

methane run is also given in Fig. 1c. As shown, the BY sample was no longer in pure fluorite phase. In addition to those belonging to δ-phase yttria-doped bismuth oxide, other XRD peaks in Fig. 1c are identified to be of cubic yttria (JCPDS file 41-1105), delta-bismuth oxide (JCPDS 27-52), and hexagonal carbon (JCPDC 19-268). Obviously, prolonged exposure to methane results in the reduction of bismuth oxide and evaporation of bismuth, which is accompanied with formation of yttria and delta phase bismuth oxide. The formation of the small amount of carbon was indicative of coking of methane. This occurred very likely in the late part of the methane-exposure period when most oxygen in the catalyst had been consumed by the reactions.

Consumption of oxygen in the BY sample when exposed to methane can be directly verified by TAG measurement. Figures 4–6 show the weight versus time curves for the BY25 samples in exposure to methane for different periods of time (at 900°C). In the period of A–B, the sample was exposed to a flow of pure oxygen. Helium was passed through the sample for 2 min prior to point B, at which the methane stream was introduced to the reactor system. There was no obvious change in the sample weight after the gas stream was switched from oxygen to helium. In Fig. 4 the sample was exposed to methane stream for 2 min (curve B–C) followed by 5-min exposure to helium stream (curve C–C′). As shown in Fig. 4, the 2-min exposure to methane stream results in about 0.3% loss in the sample weight (about 2.5% of oxygen released). The sample gained some weight after exposure to helium (curve C–C′) which contains trace impurity of oxygen (a few ppm). The sample regained its weight after exposure to an oxygen stream for 1–2 min (curve C′–D).

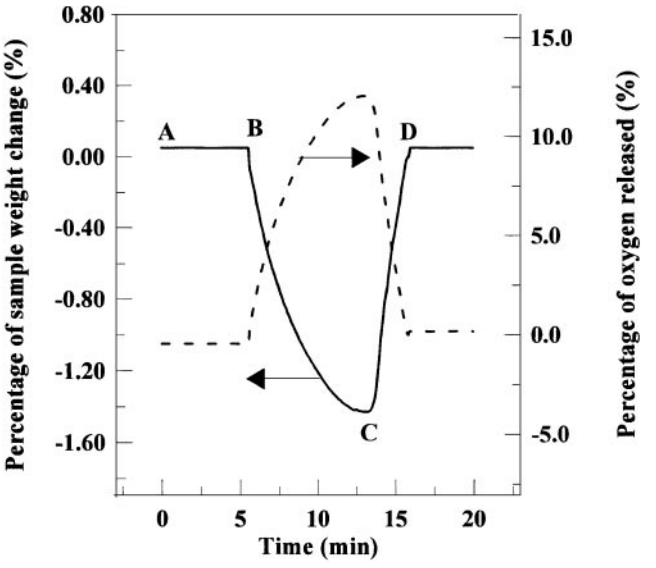

FIG. 5. Transient weight change and corresponding percentage of lattice oxygen consumed in BY25 pellets exposed to the flow of oxygen (followed with helium for 2 min) (A–B), CH_4 for 6 min (B–C), and O_2 (C–D) in TGA measurement.

The BY sample lost 1.4% of its weight (12% of oxygen released) after exposure to methane stream for 6 min (curve B–C), as shown in Fig. 5. The sample could gain its weight after reexposure to oxygen stream (curve C–D). The weight loss curves in both cases shown in Figs. 4 and 5 are similar, indicating that the oxygen release follows the same mechanism. The situation is different for the sample exposed to methane for 18 min, as shown in Fig. 6. In this case, the

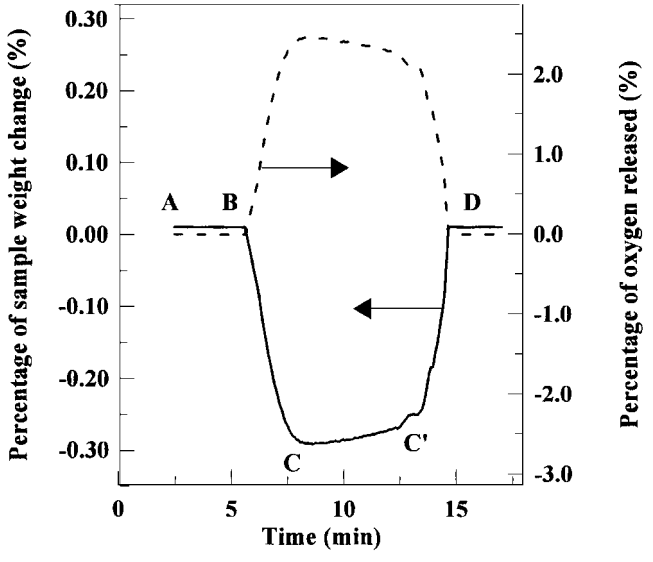

FIG. 4. Transient weight change and corresponding percentage of lattice oxygen consumed in BY25 pellets exposed to the flow of oxygen (followed with helium for 2 min) (A–B), CH_4 for 2 min (B–C), He for 5 min (C–C′), and O_2 (C′–D) in TGA measurement.

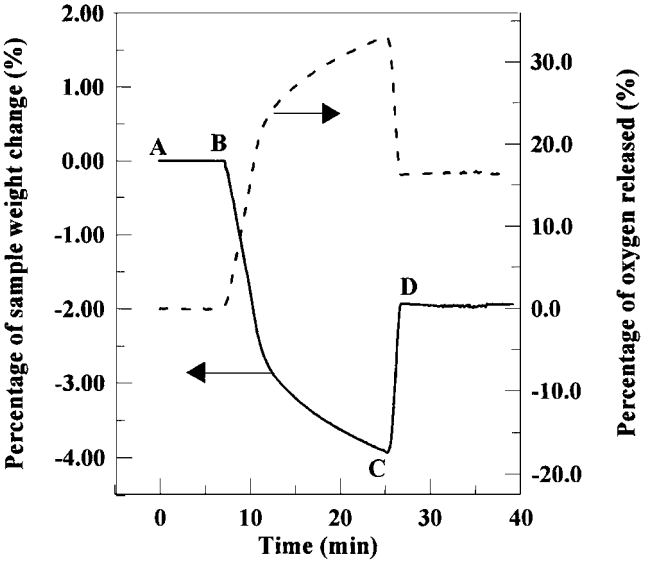

FIG. 6. Transient weight change and corresponding percentage of lattice oxygen consumed in BY25 pellet exposed to the flow of oxygen (followed with helium for 2 min) (A–B), CH_4 for 18 min (B–C), and O_2 (C–D) in TGA measurement.

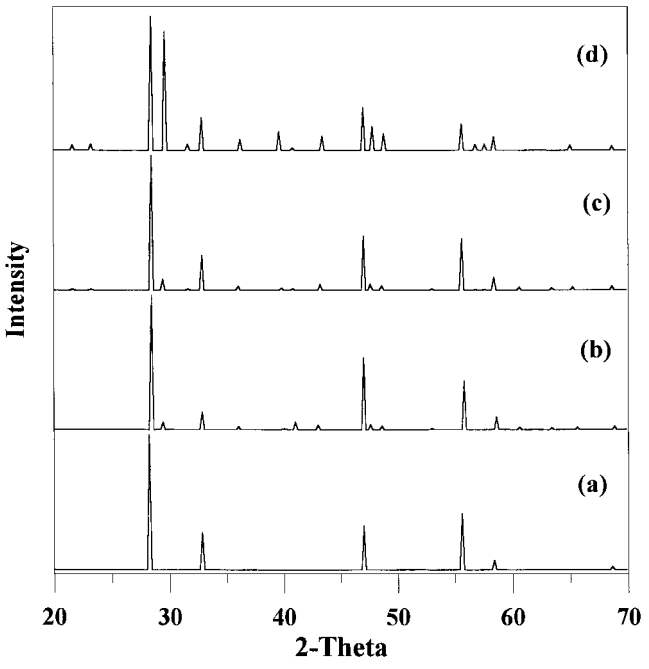

FIG. 7. XRD patterns of BY25 samples after exposed to various gas streams at 900°C: (a) after 2 h in He; (b) after 2 min in CH_4; (c) after 6 min in CH_4; and (d) after 18 min in CH_4.

sample lost 3.7% of the total weight (curve B–C) (about 33% oxygen release). This weight loss curve was characterized by a fast (up to about 20% of the oxygen released) and a slow (20%–35% of oxygen released) period. The sample could not recover its weight after reexposure to oxygen (curve C–D).

The XRD patterns of the BY samples after the above transient TGA measurements are given in Fig. 7. As shown in Figs. 7b and c, the samples with the transient data given in the Figs. 4 and 5 remained essentially in the fluorite-type fcc single phase. The percentage of oxygen released from these samples during the methane run was smaller than 20%. The sample with transient data given in Fig. 6 contained a δ-Bi_2O_3 phase and a cubic Y_2O_3 phase, as shown in Fig. 7a. Compared to the sample with the XRD pattern given in Fig. 1c (28-min exposure to methane), the BY25 sample after 18-min exposure to methane did not contain the delta phase bismuth oxide and carbon. The XRD pattern of the BY25 sample after exposure to the helium stream for 2 h at 900°C is also given in Fig. 7a for comparison. As shown, the sample remained in the perfect fluorite structure.

The above transient TGA data are consistent with the results of fixed-bed reactor measurements in the following three aspects: (1) The oxygen consumption rate curve during the methane run can be characterized by a fast period and a slow period, with the transition point at which about 20% of the oxygen is consumed (or released); (2) The BY samples having experienced less than about 20% oxygen loss could recover their weight after reexposure to oxygen and remained essentially in the same fluorite phase; (3) The BY samples having experienced more than 20% oxygen loss could not recover their weight, and part of the samples had transformed to different phases. It should be noted that the time of exposure to methane corresponding to a given amount of oxygen loss are not exactly the same for the samples placed in the fixed-bed reactor and microbalance. This is because the methane flow velocity and contact mode over the BY pellets are not identical in these two cases.

The above results can be explained by the following mechanism. A BY pellet after heating up to 900°C in oxygen (or air) contains a considerable amount of nonstoichiometric oxygen in its lattice. When exposed to methane in the first 5 min, OCM consumes primarily the nonstoichiometric oxygen stored in the BY25 pellet, as described below in the Kroger–Vink notation,

$$O_o^x + CH_4 + 2\,h^\bullet \Rightarrow V_o^{\bullet\bullet} + C_2H_y + H_2O + CO_x,$$

where O_o^x represents the lattice oxygen; $h^\bullet$, the electron-hole; $V_o^{\bullet\bullet}$, the oxygen vacancy; C_2H_y, the C_2 products; and CO_x, the carbon oxides. The reaction rate or the oxygen consumption rate in this period is determined by the *chemical* diffusion of oxygen from the bulk to the surface of the BY25 pellet. The oxygen transport rate in this case is controlled by the electron-hole conduction since BY25 is an ionic conductor with small p-type electronic conductivity in large oxygen pressure range (14).

After about 20% oxygen (nonstoichiometric oxygen) was consumed, there were about 25%-oxygen lattice sites vacant in the BY25 pellet. These oxygen vacancies in the BY25 can be filled by oxygen after reexposing the sample to oxygen as

$$V_o^{\bullet\bullet} + 0.5\,O_2 \Rightarrow O_o^x + 2\,h^\bullet.$$

This process is faster than the oxygen release process since the driving force for chemical diffusion of oxygen into the BY25 pellet is larger than that in the oxygen release process (15). The BY25 pellet sample before and after refilling of the oxygen remains in the fluorite structure.

After consumption of the nonstoichiometric oxygen, continuous exposure of the BY pellet to methane results in the consumption of the stoichiometric oxygen as

$$MO_x + CH_4 \Rightarrow M + C_2H_y + H_2O + CO_x,$$

where MO_x represents the BY25 (yttria and bismuth oxide) and M is the metal. In this period of time, OCM reactions consume oxygen and reduce the metal oxides to metals. The reduction reactions start on the outer surface of the BY25 pellet and propagate into the bulk of the pellet. The rate of the reduction reactions is smaller than the chemical diffusion of the nonstoichiometric oxygen as the former requires more energy than the latter. Part of the bismuth formed during the reduction reaction might have been evaporated at

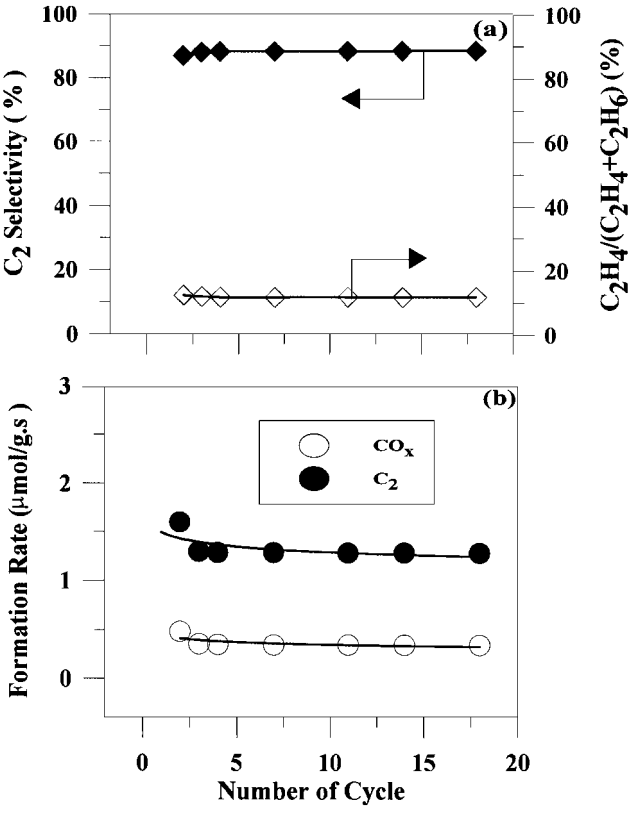

FIG. 8. C_2 selectivity, percentage of ethylene, and C_2 and CO_x formation rates as a function of number of cycles over BY25 pellets under cyclic mode.

900°C (deposition of bismuth on the tube wall of the micro electronic balance was observed in some cases). The part of the BY25 pellet that has been reduced could not restore its fluorite structure upon reexposure to oxygen.

The above experimental data suggested that for the BY25 sample studied in this work the appropriate methane contact time was about 5 min in order to maintain the same phase and chemical structure of BY25. To examine its stability against $O_2 \rightarrow CH_4 \rightarrow O_2$ cycles, OCM reactions over the BY25 pellets in cyclic operating mode with a methane run time of 4 min were performed continuously for 18 cycles. The C_2 and CO_x formation rates, C_2 selectivity and $C_2H_4/(C_2H_4 + C_2H_6)$ ratio, measured at about 0.5 min of methane run time in each cycle, are plotted against the cycle number in Fig. 8. As shown, the catalytic properties are constant throughout the 18 cycles. XRD pattern of the BY sample after the 18 cycles show that the sample still remained in the fcc δ-Bi_2O_3 phase structure.

CONCLUSIONS

The phase structure, chemical stability, and OCM catalytic properties of δ-phase 25 mol% yttria-doped bismuth oxide (BY25) pellets under methane atmosphere at high temperatures were studied by XRD, transient TGA, and fixed-bed reactor measurements. A BY25 pellet presaturated with oxygen can maintain its fluorite-type phase structure and OCM catalytic properties within about 5 min exposure to pure methane. In this period OCM reactions consume only nonstoichiometric oxygen (<20% of the total oxygen), and the catalytic properties and sample weight of the BY25 can be restored by reexposing the BY25 pellets to oxygen.

Prolonged (>5–7 min) exposure of BY25 to methane at high temperatures results in loss of stoichiometric oxygen in the catalyst. The OCM reaction rates in this period, although with a high selectivity, are lower than those in the initial period. Part of metal oxides in the BY25 pellets is reduced. The sample weight and phase structure of the reduced BY25 sample cannot be restored by reexposing the sample to oxygen. If the methane exposure time is kept within 5 min, the fluorite-type BY25 can maintain its phase structure and OCM catalytic properties at least for 18 cycles of exposure to methane and oxygen.

The results suggest that BY25 is stable for the OCM reaction, as long as sufficient nonstoichiometric oxygen is available in the BY25 pellets for OCM. This finding is important for the membrane reactor application of BY25 in which one surface of the BY25 membrane is exposed to methane (or another hydrocarbon) and the other to oxygen (or air). The stability and catalytic properties of the BY25 membrane surface in the reaction side can be maintained if sufficient oxygen is continuously provided from the other side of the membrane.

ACKNOWLEDGMENT

This project was supported by the National Science Foundation (CTS-9502437, Career Award).

REFERENCES

1. Bouwmeester, H. J. M., and Burggraaf, A. J., Dense ceramic membranes for oxygen separation, *in* "The CRC Handbook of Solid State Electrochemistry" (P. J. Gellings and H. J. M. Bouwmeester, Eds.), Chap. 14 (CRC Press, New York, 1997).
2. Tillement, O., Solid state ionics electrochemical devices, *Solid State Ionics* **68**, 9 (1994).
3. Zeng, Y., and Lin, Y. S., Catalytic properties of yttria doped bismuth oxide ceramics for oxidative coupling of methane, *Appl. Catal. A* **159**, 101 (1997).
4. Zeng, Y., and Lin, Y. S., Oxidative coupling of methane on oxygen-semipermeable yttria-doped bismuth oxide ceramics in a reducing atmosphere, *Indus. Eng. Chem. Res.* **36**, 277 (1997).
5. Wang, W., and Lin, Y. S., Analysis of oxidative coupling of methane in dense oxide membrane reactor, *J. Membrane Sci.* **103**, 219 (1995).
6. Lin, Y. S., and Zeng, Y., Catalytic properties of oxygen semipermeable perovskite type ceramic membrane materials for oxidative coupling of methane, *J. Catal.* **64**, 220 (1996).
7. Dordor, P. J., Tanaka, J., and Watanabe, A., Electrical characterization of phase transition in yttrium doped bismuth oxide, $Bi_{1.55}Y_{0.45}O_3$, *Solid State Ionics* **25**, 177 (1987).
8. Watanabe, A., Is it possible to stabilize δ-Bi_2O_3 by an oxide additive?, *Solid State Ionics* **40/41**, 889 (1990).

9. Joshi, A. V., Kulkarni, S., Nachlas, J., Diamond, J., Weber, N., and Virkar, A.V., Phase stability and oxygen transport characteristics of yttria- and niobia-stabilized bismuth oxide, *J. Mat. Sci.* **25**, 1237 (1990).
10. Kruidhof, H., de Vries, K. J., and Burggraaf, A. J., Thermochemical stability and nonstoichiometry of yttria-stabilized bismuth oxide solid solutions, *Solid State Ionics* **37**, 2131 (1990).
11. Kruidhof, H., Bouwmeester, H. J. M., de Vries, K. J., Gellings, P. J., and Burggraaf, A. J., Thermochemical stability and nonstoichiometry of erbia-stabilized bismuth oxide, *Solid State Ionics* **50**, 181 (1992).
12. Amenomiya, Y., Birss, V. I., Goledzinowski, M., Galuszka, J., and Sanger, A. R., Conversion of methane by oxidative coupling, *Catal. Rev.-Sci. Eng.* **32**, 163 (1990).
13. Alcock, C. B., Carberry, J. J., Doshi, R., and Gunasekaran, N., Methane coupling reaction on oxide solid solution catalysts, *J. Catal.* **143**, 533 (1993).
14. Lin, Y. S., Wang, W., and Han, J., Oxygen permeation through thin mixed-conducting solid oxide membranes, *AIChE J.* **40**, 786 (1994).
15. Zeng, Y., and Lin, Y. S., A tranisent TGA sudy on oxygen permeation properties of perovskite type ceramics, *Solid State Ionics* **110**, 209 (1998).